Design of Primary and Secondary Cells : II . An Equation Describing Battery Discharge

C. M. Shepherd

J. Electrochem. Soc. 1965, Volume 112, Issue 7, Pages 657-664.
doi: 10.1149/1.2423659

Design of Primary and Secondary Cells

II. An Equation Describing Battery Discharge

C. M. Shepherd

U. S. Naval Research Laboratory, Washington, D. C.

ABSTRACT

A discussion is given of the derivation and application of an equation which gives an excellent description of a wide variety of cell and battery discharges. This equation gives the cell potential during discharge as a function of discharge time, current density, and certain other factors. It makes possible a complete description of cell discharge characteristics, using a minimum of experimental data and at the same time pinpointing experimental errors. It can also be used to describe cell charges, capacities, power evolution, and to predict capacities. A description is given of a simple numerical method for fitting this equation to a particular set of battery discharge curves. A graphical method is described for comparing characteristics of various types of cells.

This paper is one of a series whose ultimate goal is to determine procedures for designing batteries having optimum properties such as minimum weight or minimum volume. In particular, the derivation and application of an equation describing cell discharge will be discussed. The equation can be used to locate variations in the discharge data due to experimental error, uncontrolled variables, etc., thus minimizing the amount of experimental data needed and cutting the costs of evaluation. A complete set of discharge curves can be described by a single equation, making it possible to present in less space a more detailed description of cell characteristics than has been customary in many battery papers.

Derivation and Determination of the Discharge Equation

The mathematical analysis given here is based on the assumption that the following conditions are applicable: (*A*). The anode and/or cathode have porous active materials. (*B*). The electrolyte resistance is constant throughout discharge. (*C*). The cell is discharged at a constant current. (*D*). The polarization is a linear function of the active material current density.

When ionic discharge is the slow or rate determining process, the relationship between steady-state current density and activation overpotential at an electrode in a constant concentration electrolyte is usually written as

$$i = i_o e^{\alpha\eta ZF/RT} - i_o e^{-(1-\alpha)\eta ZF/RT} \qquad [1]$$

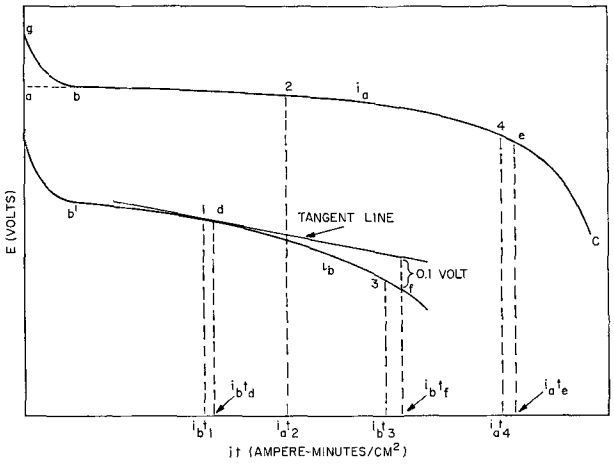

Fig. 1. Typical discharge curves used in equation fitting

where i is the apparent current density in amperes per square centimeter, i_o is the apparent exchange current density in amperes per square centimeter, α is the transfer coefficient ($0 \leq \alpha \leq 1$), Z is the number of electrons transferred in the rate-determining step, F is the Faraday, R is the gas constant, and T is the temperature in °K. The steady-state activation overpotential, η, is positive for the deposition of cations.

When the exponential terms are expanded as a series, powers greater than one can be neglected if η is sufficiently small and Eq. [1] becomes

$$\eta = \left(\frac{RT}{ZFi_o}\right) i \qquad [2]$$

thus establishing a linear relationship between η and i which is fairly accurate up to the values of η equal to approximately 0.03v. If Eq. [1] is applicable to a cell, the variation of η with change in i can be fitted by a straight line within approximately 0.02-0.04v up to values of η equal to about 0.2-0.4v. A potential drop of this magnitude would cover the major portion of the polarization that occurs during most battery discharges.

In Fig. 1, two solid curves, i_a and i_b, are shown which represent typical battery discharges. The potential in volts is plotted as a function of (it), the quantity of electricity that has been obtained from the battery at time t. It is assumed in the derivation that follows that the polarization is linear to the right of point b and b'. If all factors except polarization are ignored, then E_c, the cathode potential during discharge, is defined as

$$E_c = E_{sc} - K_c i_{am} \qquad [3]$$

where E_{sc} is a constant potential, K_c is the cathode coefficient of polarization per unit active material current density, and i_{am} is the active material current density. The successful use of Eq. [3] as a fundamental equation in the derivation that follows does not necessarily imply that the theoretical factors associated with Eq. [1] apply to most battery discharges even though both equations are linear.

In the case of a porous electrode the active material current density i_{am} is defined as being inversely proportional to the amount of unused active material and is also equal to i at the beginning of the discharge. Consequently

$$i_{am} = \left(\frac{Q_c}{Q_c - it}\right) i \qquad [4]$$

where t is the time at any point during the discharge and Q_c is the amount of available cathode active material expressed in units such as ampere hours per unit area.

When Eq. [4] is substituted in Eq. [3]

$$E_c = E_{sc} - K_c\left(\frac{Q_c}{Q_c - it}\right)i \qquad [5]$$

Similarly

$$E_a = E_{sa} - K_a\left(\frac{Q_a}{Q_a - it}\right)i \qquad [6]$$

where the subscripts a and c denote the anode and cathode values for the constants, respectively. A sign convention is used here which makes the value of the potential terms positive.

If Q_a is approximately equal to Q_c, as it generally is in a well designed cell, Eq. [5] and [6] can be summed to give

$$E = E_s - K\left(\frac{Q}{Q - it}\right)i \qquad [7]$$

where $E = E_a + E_c$ is the potential of the cell (neglecting the internal resistance) at any time t during the discharge; $E_s = E_{sa} + E_{sc}$ is a constant potential; $K = K_a + K_c$ is the polarization coefficient in ohm cm^2; and $Q = Q_a = Q_c$ is the available amount of active material in coulombs or similar units per unit area.

If Q_a is appreciably larger than Q_c, then the numerical increase in the value of the last term in Eq. [6] will be small compared to the numerical increase in the value of the last term of Eq. [5] as (it) approaches Q_c in value. Consequently, the second term of Eq. [6] can be considered to be approximately constant and the sum of Eq. [5] and [6] will still have approximately the form shown in Eq. [7]. Under these conditions the approximate values of K, Q and E_s will be $K = K_c$, $Q = Q_c$, and $E_s = E_{sa} + E_{sc} - K_a i$. If Q_c is appreciably larger than Q_a, then the approximate values of K, Q, and E_s will be $K = K_a$, $Q = Q_a$, and $E_s = E_{sa} + E_{sc} - K_c i$. Thus Q is determined by the amount of available active material on the controlling electrode which is the one that fails first. A similar argument will show that the same type of equation will be approximately true when several cells are connected in series to form a battery.

When the potential drop due to internal resistance is considered, Eq. [7] becomes

$$E = E_s - K\left(\frac{Q}{Q - it}\right)i - Ni \qquad [8]$$

where N, the internal resistance per unit area, is measured in ohm cm^2 or other suitable units.

When Eq. [8] is evaluated mathematically, a set of curves is obtained, one of which, plotted in Fig. 1, is a dotted line from a to b and a solid line from b to c. The initial drop in potential at the beginning of a cell discharge is not included in Eq. [8]. Consequently another term must be added to correct for the difference between the dotted line potential calculated from Eq. [8] and the solid line gb that represents the actual discharge potential. It has been found that the expression $A\exp(-BQ^{-1}it)$, where A and B are empirical constants, gives an excellent estimate of the initial potential drop in virtually every case. When this term is added to Eq. [8], the final equation

$$E = E_s - K\left(\frac{Q}{Q - it}\right)i - Ni + A\exp(-BQ^{-1}it) \qquad [9]$$

is obtained. In a number of cases the initial drop in potential was too rapid to be included in the observed experimental data and consequently, the value of $A\exp(-BQ^{-1}it)$, being negligible, could be ignored.

That portion of the discharge curve that lies to the right of point b in Fig. 1 could be predicted from Eq. [9] if the numerical values of E_s, K, Q, and N were known, providing the basic assumptions were true. However, the labor involved in determining these values would be so large that it probably would be easier, and certainly more accurate, to determine discharge curves experimentally. However, Eq. [9] can be fitted numerically to experimental discharge data, thus determining empirical values of E_s, K, Q, N, A, and B. Such a numerical equation gives an accurate description of the cell or battery discharge and can be used to describe energy evolution, cell capacity, and can be used in predicting cell capacities. Despite its successful applications, it must be considered to be an empirical equation since the numerical values of K, Q, and N that are determined in this manner will vary considerably at times from their true values as defined in the basic assumptions.

There are a number of methods that can be used to determine the numerical values of E_s, K, Q, N, A, and B in Eq. [9] from experimental discharge data, most of which are unsuitable. The least squares solution is particularly involved and time-consuming. The following approach is easily applied, rapid, reasonably accurate and is used in fitting Eq. [9] to discharge curves obtained at a number of current densities. In Fig. 1, four points, labeled 1, 2, 3, and 4 have been selected on two discharge curves which were obtained at the moderately low current density, i_a, and the moderately high current density, i_b. The values of E and (it) at points 1, 2, 3, and 4 are E_1, E_2, E_3, and E_4 and i_bt_1, i_at_2, i_bt_3, and i_at_4, respectively. These four points are chosen to the right of the initial potential drop. Thus the value of $A\exp(-BQ^{-1}it)$ is negligible and the potential at point 2 is found from Eq. [9] to be approximately

$$E_2 = E_s - K\left(\frac{Q}{Q - i_at_2}\right)i_a - Ni_a \qquad [10]$$

Similarly

$$E_4 = E_s - K\left(\frac{Q}{Q - i_at_4}\right)i_a - Ni_a \qquad [11]$$

Subtracting Eq. [11] from Eq. [10] gives

$$E_2 - E_4 = Ki_a\left(\frac{Q(i_at_4 - i_at_2)}{(Q - i_at_1)(Q - i_at_2)}\right) \qquad [12]$$

The equation for $E_1 - E_3$ is obtained in a similar manner and is divided into Eq. [12] to give

$$\frac{E_2 - E_4}{E_1 - E_3} = \frac{i_a}{i_b}\,\frac{(i_at_4 - i_at_2)}{(i_bt_3 - i_bt_1)}\,\frac{(Q - i_bt_3)(Q - i_bt_1)}{(Q - i_at_4)(Q - i_at_2)} \qquad [13]$$

When numerical values of E, i, and (it) are taken from the discharge data in Fig. 1 and substituted in Eq. [13], a quadratic equation in Q is obtained which is solved to give a numerical value of Q. This value of Q is substituted in Eq. [12] and solved to obtain a numerical value of K. When these values of Q and K are substituted in Eq. [10] and a similar equation for E_1, two simultaneous equations are obtained which may be solved to give numerical values for E_s and N. When these values of E_s, N, K, and Q are substituted in Eq. [9], E is obtained as a specific function of (it). The calculation of Q by use of Eq. [13] can generally be simplified by choosing point 2 in a manner such that i_at_2 equals either i_bt_3 or i_bt_1.

The two discharge curves, i_a and i_b, that are chosen as a basis for these calculations should be representative of the complete set of discharge curves and should show no obvious visual discrepancies that would indicate variations not present in the other curves. They are selected in the following manner. If (it) is held constant, Eq. [9] shows that the potential E to the right of point b in Fig. 1 may be stated as a linear function of the current density, i, in the form

$$E = E_s - B_1 i \qquad [14]$$

where B_1 is a constant equal to $K\left(\frac{Q}{Q - it}\right) + \mathrm{N}$

A fairly good fit to Eq. [14] is shown in Fig. 2 where E has been plotted as a function of i for five values of

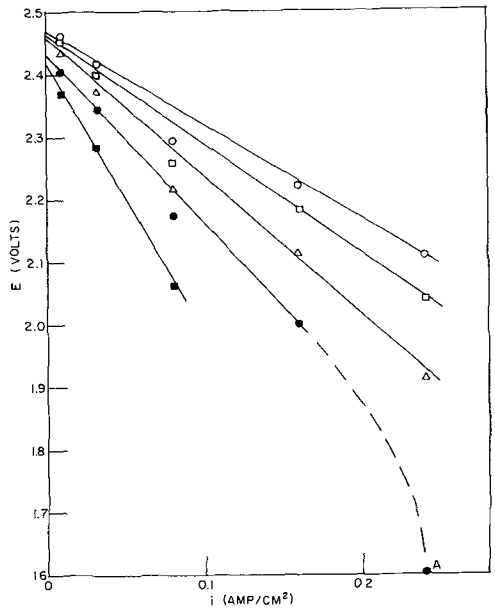

Fig. 2. Potential during cell discharge *vs.* current density for constant values of (*it*). The *it* values in amp-hr/cm²: ○, 0.00266; □, 0.00532; △, 0.00798; ●, 0.01063; ■, 0.01329.

(*it*) using the discharge data for the lead-zinc cell shown in Fig. 4g. The potentials, E at the current density, $i = 0.0798$ amp/cm², were considerably lower than the straight lines drawn through the corresponding values of (*it*), thus showing that this particular discharge was out of agreement with the remainder of the data. Variations this large were not observed as a rule. The remaining four values of i gave good straight line fits in Fig. 2. Either of the two low values of i could be used for i_a and either of the two high values could be used for i_b. As a rule a plot of E *vs.* i for each of two values of (*it*) will be sufficient to select satisfactory values of i_a and i_b. Points such as A which were taken past the knee of the discharge curve should not be used in making up these charts of E *vs* i. Very low values and very high values of i are avoided if feasible in selecting i_a and i_b since these extreme values have a tendency to be less accurate. With a little experience, i_a and i_b often can be selected on the basis of judgment without drawing up a chart such as that shown in Fig. 2.

If Eq. [9] is a perfect fit for the discharge data, then the plot of E *vs.* i as illustrated in Fig. 2 would consist of straight lines intersecting on the E axis at $E = E_s$. If the plot of E *vs.* i gives lines that do not intersect on the E axis or if they are curves, then Eq. [9] does not describe the discharge data perfectly. However, Eq. [9] is so adaptable that it can describe such cases with good accuracy and it has not been necessary to reject any data on this account. Discharge data were not accepted for study here whenever they were so erratic and full of error that a plot of E *vs.* i did not give some semblance of a smooth curve. It was found that all of the data that were acceptable on this basis could be fitted by Eq. [9]. Virtually all of the room temperature discharge data taken from the literature were found to be acceptable. At low temperatures the available data were more erratic and less acceptable.

The points 1, 2, 3, and 4 used to calculate the numerical values of the parameters K, Q, and N are selected in the manner illustrated in Fig. 1. A tangent is drawn to the high current density discharge curve at point d and point f is selected to be 0.1v below the tangent line. Point d is determined by eye by laying a transparent plastic straight edge tangent to the curve and adjusting the point of tangency until $i_b t_d$ equals 0.5 $i_b t_f$. This method is rapid and sufficiently accurate. Point e is located in a manner similar to f. The value of E for point 3 is approximately 0.03v

Table I. Values of ΔE in volts

	(*i t*)						
i	2	5	10	20	30	50	65
2	0.116	0.106	0.091	0.068	0.045	0.019	0.007
10	0.133	0.118	0.088	0.057	0.037	0.013	0.002
20	0.145	0.123	0.087	0.050	0.032	0.008	0.000
40	0.144	0.120	0.084	0.048	0.027	0.006	0.000
60	0.141	0.117	0.087	0.056	0.030	0.008	0.002
80	0.140	0.115	0.086	0.056	0.031	0.003	0.001
100	0.143	0.123	0.085	0.049	0.026	0.009	0.003
120	0.153	0.118	0.085	0.049	0.025	0.010	0.000
Avg.	0.139	0.118	0.087	0.054	0.032	0.0095	0.0018

greater than it is for point f. The value of E for point 4 is approximately 0.02v greater than it is for point e. Point 1 is chosen so $i_b t_1$ equals approximately 0.5 $i_b t_3$. If $i_b t_f / i_a t_e$ is less than 0.7, point 2 is chosen directly above point 3 so that $i_a t_2$ will equal $i_b t_3$. If $i_b t_f / i_a t_e$ is greater than 0.7, point 2 is chosen directly above point 1 so that $i_a t_2$ will equal $i_b t_1$. This procedure gives an approximate location of the points which supply the numerical data to substitute in Eq. [12] and [13], and make possible the calculation of numerical values of K, Q, N, and E_s which can be substituted in Eq. [9] along with values of A and B to give a fairly good numerical description of the discharge data. Values of E *vs.* (*it*) for different discharge rates can be calculated from this numerical equation and compared to the actual discharge data. If the agreement is not good enough, it can be improved by the method of successive approximations. A new calculation can be made using slightly different locations for one or more of the four points on the two discharge curves, i_a and i_b. If the calculated points were too far away from the measured results in the area to the left of some point such as 4, it could be corrected by selecting a new location for point 4 which would be slightly to the left of the old location and calculating a new numerical equation. The points calculated by this new equation to the right of point 4 would be a little farther away from the actual discharge data as a rough rule than those calculated from the first equation. A fairly good fit should be obtained with the first calculated equation. If it is at all possible, a very good fit will have been obtained by the third calculation. Each calculation should take less than one hour of time.

The calculations thus far are sufficient to give a numerical evaluation of Eq. [8], which is plotted in Fig. 1 as a dotted line from a to b and a solid line from b to c. The difference in potential, ΔE, between this calculated dotted line of Eq. [9] and the true discharge potential shown by the solid line gb in Fig. 1 is approximated by the term $A \exp(-BQ^{-1}it)$ in Eq. [10]. In Table I values of ΔE *vs. it* are given for each discharge curve of the Edison cell shown in Fig. 4a. The average values of ΔE *vs.* (*it*) in Table I are plotted on semi log paper in Fig. 3 and fitted by a straight line

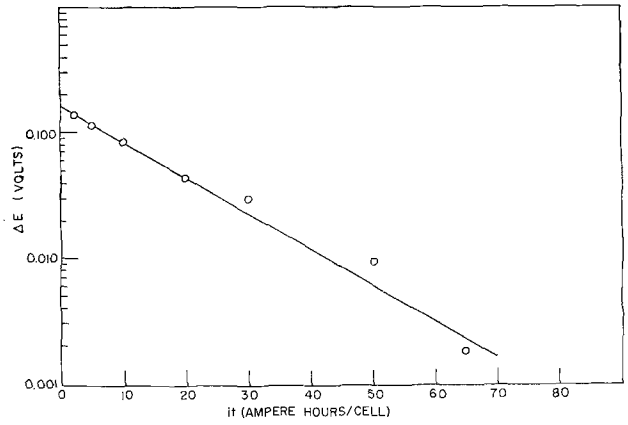

Fig. 3. Determination of ΔE from numerical data

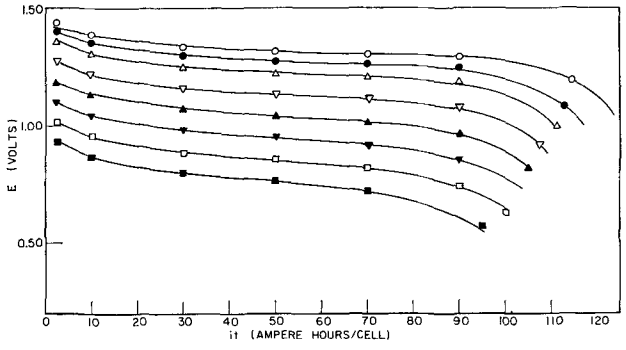

Fig. 4a-g. Comparison of points calculated from discharge equations with solid lines representing actual discharges at various current densities. a. Edison cell, NiOOH-Fe-KOH. Calculated points, amp/cell: ○, 2; ●, 10; △, 20; ▽, 40; ▲, 60; ▼, 80; □, 100; ■, 120.

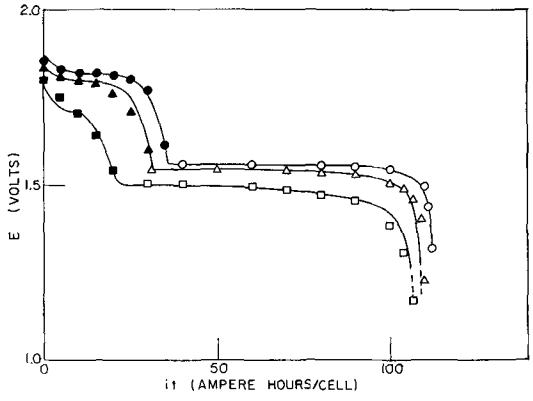

Fig. 4b. Silver cell, AgO-Zn-KOH. Calculated points, amp/cell: ●—○, 2.5; ▲-△, 10; ■-□, 60.

whose equation is $\Delta E = A\exp(-BQ^{-1}it)$. The intercept on the ordinate gives the numerical value of A. The numerical value of B/Q can be calculated from the slope or from a single point taken on the straight line. In nearly all cells the value of ΔE is much less at high values of it/Q than in the example shown in Fig. 3 where $\Delta E = 0.006$v at it equals 50 or it/Q equals 0.433. In most cells ΔE would be less than 0.006v at a value of it/Q equal to 0.10 and would be close to zero in value at it/Q equals 0.15. If points 1 and 2 were chosen in Fig. 4a at $it = 50$ then a correction of $\Delta E = 0.006$v should be subtracted from the values of E_1 and E_2 to be used in calculating the constants in Eq. [9]. This value of ΔE could not be estimated accurately until after the first calculation had been made.

Discussion of the Equation and its Applications

Experimental discharge data for a number of different types of batteries have been plotted as solid lines in Fig. 4 (1, 2, 3, 4, 5). The potential E is shown for various current densities, i, as a function of (it) which is expressed in ampere hours per square centimeter or ampere hours per cell where the area is not known. Equation [9] has been fitted numerically to each set of discharge data thus obtaining a different numerical equation for each chart in Fig. 4. The numerical values of the constants for each of these equations are shown in Table II and are dependent on the unit of time, t, and also on the unit of area used in defining the current density. Since the area is unknown in most cases, the area of the entire cell is

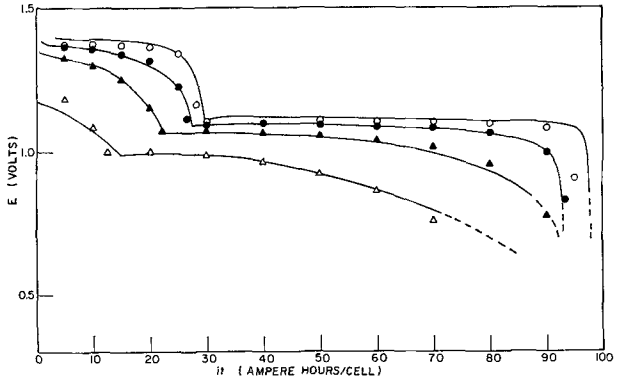

Fig. 4c. Silver cadmium cell, AgO-Cd-KOH. Calculated points, amp/cell: ○, 0.625; ●, 2.5; ▲, 10.0; △, 40.0.

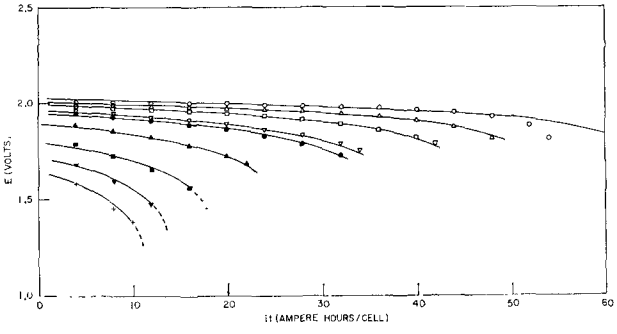

Fig. 4d. Lead acid cell, PbO_2-Pb-H_2SO_4. Calculated points, amp/cell: ○, 0.8; △, 2; □, 4; ▽, 8; ●, 10; ▲, 20; ■, 40; ▼, 60; +, 80.

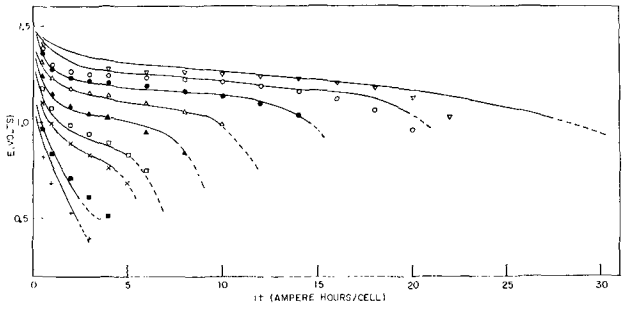

Fig. 4e. Dry cell. Calculated points, amp/cell: ▽, 0.125; ○, 0.25; ●, 0.5; △, 1.0; ▲, 2.0; □, 3.0; X, 4.0; ■, 6.0; +, 8.0.

Table II. Values of the parameters in Eq. [9] for various types of cells

Type cell	Fig. No.	E_s, v	K, ohm cell*	Q, amp-hr/cell*	N, ohm cell*	A, v	B/Q Cell*(amp-hr)$^{-1}$	Temp, °C	Ref.
Edison	4a	1.3080	0.0003936	115.4	0.00390	0.165	0.06564	Room	1
Silver-zinc	$4b_1$	1.8310	0.005138	37.06	−0.00388	0.020	0.60	27	2
	$4b_2$	1.5567	0.00040	112.0	0.00067			27	2
Silver-cadmium	$4c_1$	1.3733	0.00831	28.68	−0.00543			27	
	$4c_2$	1.0990	0.00260	95.75	−0.000965			27	
Lead acid	4d	2.0030	0.0189	58.31	−0.0150			25	3
Dry cell	4e	1.2743	0.3343	25.61	−0.269	0.360	2.197	25	
Ni-Cd	4f	1.2021	0.001358	74.67	−0.000241	0.080	0.1386	−18	4
Lead-zinc	4g*	2.4607	0.9722	0.01737	0.3589			27	5

* The word cell is defined as the electrode area of the entire cell. It is replaced in 4g by cm². Since the area terms cancel out in Eq. [9], it is not necessary to know the numerical value of the area.

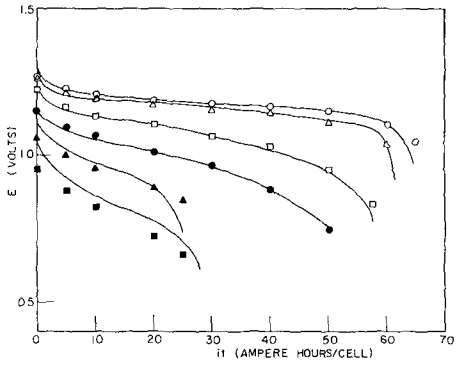

Fig. 4f. Sintered nickel cadmium cell, NiOOH-Cd-KOH, —18°C. Calculated points, amp/cell: ○, 15; △, 24; □, 65; •, 120; ▲, 200; ■, 300.

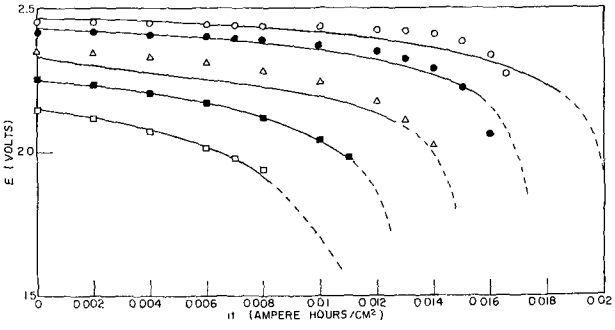

Fig. 4g. PbO_2-Zn-H_2SO_4 reserve cell. Calculated points, amp/cm²: ○, 0.00957; •, 0.0319; △, 0.0798; ■, 0.1595; □, 0.2393.

taken as the unit area and the current density is defined as the amperes per cell and is equal in value to the total discharge current. The points in Fig. 4 are calculated from these equations. It can be seen that the calculated points give good fits in every case to the solid lines that represent the actual discharge data. Thus the information in Table II is sufficient to give an excellent description of the discharge data in Fig. 4 at a considerable savings in space. Equation [9] was applied to a wide variety of discharge data from various types of physically constructed batteries for each of the common battery systems. The examples selected for Fig. 4 were in each case the one which covered the widest range of current densities. Equation [9] was also fitted successfully to discharge data from the following systems: PbO_2-Cd-H_2SO_4, HgO-In-KOH, air cell-air-Zn-KOH, AgCl-Zn-NaCl, PbO_2-Pb-$HClO_4$, CuO-Zn-NaOH, NiOOH-Zn-KOH, Cl_2-Zn-$ZnCl_2$, PbO_2-Sn-$HClO_4$, PbO_2-Pb-HBF_4, HgO-Zn-KOH. No individual curves were omitted in any case. The poorest fit obtained in all the cases studied was with the dry cell data which is shown in Fig. 4e. Most of the data was taken from the literature and was selected to cover as wide a range of current densities as possible. Unfortunately, the amount of low temperature discharge data was limited and some of it had to be rejected as erratic when tested by the method illustrated in Fig. 3.

In Fig. 4b and 4c the discharge took place in two steps and it was found that a separate equation could be fit to each step. The first step in each case is indicated by the subscript 1 on the figure number in Table II. For example, the equation for the silver cell in Fig. 4b would be

$$E = 1.8310 - 0.005138\left(\frac{37.06}{37.06 - it}\right) i + 0.00388\, i + 0.020 \exp(-0.60\, it)$$

or

$$E = 1.5567 - 0.0004\left(\frac{112}{112 - it}\right) i - 0.00067\, i$$

whichever is higher in value.

Whenever the calculated values of E_s, K, Q, and N are the true or defined values and are not affected by the choice of the four points, Eq. [9] fits that particular discharge data theoretically. Whenever the calculated values of E_s, K, Q and N are not the true or defined values and are affected by the choice of points 1 to 4, Eq. [9] is fitting that particular discharge data empirically. In this latter case, there are a number of specific combinations of numerical values of E_s, K, Q and N which will give good fits to a particular set of discharge curves. Among these combinations E_s and Q will be fairly constant while K and N may vary somewhat, N becoming smaller as K becomes larger. For example, two individuals fitting Eq. [9] to a particular set of discharge curves might get two different equations, each of which fit the data quite well even though they had appreciably different values for K and N.

As a very rough rule, a closer approach to a theoretical fit is generally found in the presence of one or more of the following conditions: the discharge data covers a narrow range of current densities, the potential drop due to polarization is low, the electrolyte does not change in composition during discharge, the slope of the discharge curves before the knee is relatively small, the ratio $(it)/Q$ is fairly large and covers a relatively narrow range of values of (it), and the calculated value of N is not negative. Most of these conditions can be observed in Fig. 4a.

In any case, Eq. [9] is so adaptable that wide variations in its constants, particularly K and N, enable it to be fitted with good accuracy to a very wide range of discharge data. A large increase in the numerical value of K will be accompanied by such a large decrease in the value of N that N will often be negative in value as can be seen in Table II. Since N is the internal resistance in the original derivation and theoretically cannot be negative in value, it is obvious that Eq. [9] must be considered to be empirical in most of its curve fitting applications and there is no reason to believe that it should have to describe fully the discharge of every type of battery.

In Fig. 2 the measured potential is low for the points at i equals 0.0798 amp/cm². In Fig. 4g the measured potential at this current density is appreciably lower than the calculated potential thus indicating the very strong likelihood of an error in this data. When there are only three discharge curves and two of them are correct, it is not possible to tell by this method which one of the three is in error without collecting more data. A fourth discharge made at a different current density will, if correct, determine which of the other three curves contains the error.

An examination of all of the data fitted by Eq. [9] shows that the differences between the calculated and the measured results are often larger at the highest current densities than they are at intermediate current densities. This larger variation can be attributed to the high relative dispersion of the data; the fact that the highly simplified calculation methods given here tend to give the poorest fit at high current densities; and the fact that the poorest fit is often obtained at the extreme limits when fitting equations to measured data. There is also a tendency for a very few of the calculated curves at the lowest current density to have less slope and a smaller capacity than the observed data. This condition is most noticeable in Fig. 4g and seems to be most generally associated with batteries whose electrolytes change appreciably in concentration during discharge. As a rough empirical approximation, it is assumed that the drop in potential in a battery is directly proportional to the change in electrolyte concentration during discharge, assuming all other factors are neglected. Equation (9) can then be written as

$$E = E_s - K\left(\frac{Q}{Q - it}\right) i - Ni + A \exp(-BQ^{-1}it) - Cit \quad [15]$$

where C is a constant.

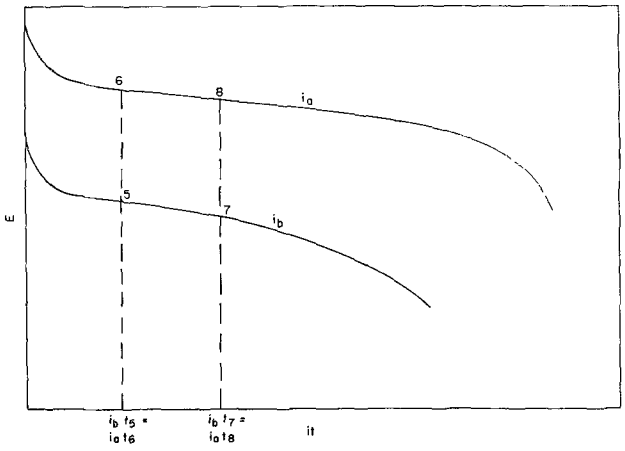

Fig. 5. Typical discharge curves to be used in numerical calculation of C.

To determine the numerical value of C select four points as shown in Fig. 5 which are far enough past the initial potential drop for the exponential term to be negligible. From Eq. [15]

$$E_5 = E_s - Ki_b\left(\frac{Q}{Q - i_b t_5}\right) - Ni_b - Ci_b t_5 \quad [16]$$

and

$$E_7 = E_s - Ki_b\left(\frac{Q}{Q - i_b t_7}\right) - Ni_b - Ci_b t_7 \quad [17]$$

Subtracting Eq. [17] from Eq. [16] gives

$$E_5 - E_7 = Ki_b\left[\left(\frac{Q}{Q - i_b t_7}\right) - \left(\frac{Q}{Q - ibt_5}\right)\right] + C(i_b t_7 - i_b t_5) \quad [18]$$

Similarly

$$E_6 - E_8 = Ki_a\left[\left(\frac{Q}{Q - i_b t_7}\right) - \left(\frac{Q}{Q - ibt_5}\right)\right] + C(i_b t_7 - i_b t_5) \quad [19]$$

From Eq. [18] and Eq. [19]

$$C = \frac{i_b(E_6 - E_8) - i_a(E_5 - E_7)}{(i_b - i_a)(i_b t_7 - i_b t_5)} \quad [20]$$

Numerical values of C are calculated from Eq. [20] and substituted in Eq. [15].

Let $E' = E + Cit$.

Then $E_1' = E_1 + Ci_b t_1$, $E_2' = E_2 + Ci_a t_2$, $E_3' = E_3 + Ci_b t_3$, and $E_4' = E_4 + Ci_a t_4$. If E_1', E_2', E_3', and E_4' are substituted for E_1, E_2, E_3, E_4, respectively, in Eq. [10] to [13], they can be used to calculate numerical values of Q, K, N, and E_s in the manner previously described.

Numerical values of Eq. [15] were determined in this manner for the lead-zinc cell shown in Fig. 4g and found to be

$$E = 2.4775 - 0.9237\left(\frac{0.0181}{0.0181 - it}\right)i - 0.4295\,i - 4.25\,it$$

Calculated points from this equation are shown in Fig. 6 to give a better fit to the experimental data than was obtained by the use of Eq. [9].

If the basic assumptions are assumed to be true during the charge of a cell, then the following equation would hold for the potential during charge

$$E = E_s + K\left(\frac{Q}{Q - it}\right)i + Ni - A\exp(-BQ^{-1}it) \quad [21]$$

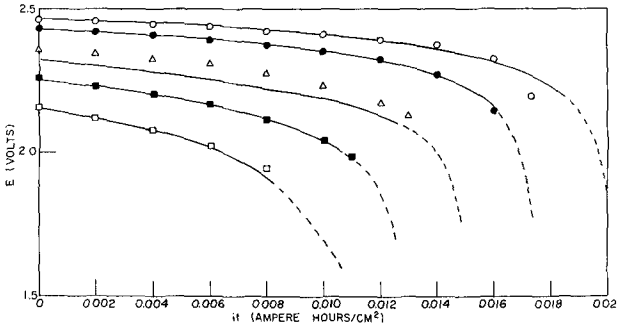

Fig. 6. Comparison of points calculated from the discharge equation with solid lines representing actual discharges at various current densities. PbO_2-Zn-H_2SO_4 reserve cell. Calculated points, amp/cm²: ○, 0.00957; ●, 0.0319; △, 0.0798; ■, 0.1595; □, 0.2393.

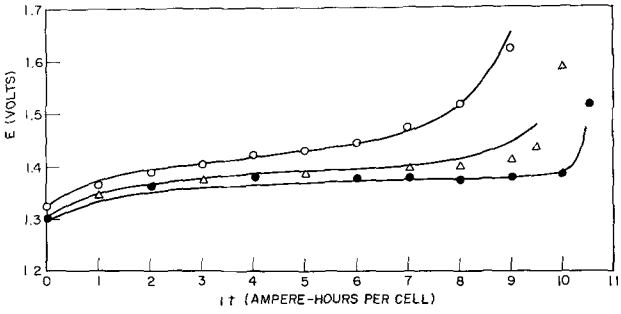

Fig. 7. Comparison of the charge data of a Ni-Cd cell with the calculated results for various current densities. Nickel cadmium cell, Ni-OOH-Cd-KOH. Calculated points, amp/cell: ○, 16.0; △, 2.5; ●, 0.16.

Equation [21] can be obtained from Eq. [9] by reversing the signs of the last three terms. Equation [21] has been fitted to the charge of a Ni-Cd cell in Fig. 7. The solid lines represent the actual data and the points are calculated from the equation

$$E = 1.379 + 0.0024\left(\frac{1}{1 - 0.095\,it}\right)i - 0.00116\,i - 0.08\exp(-0.693\,it)$$

The use of Eq. [21] in describing the charging of a cell has been tested on a very limited amount of data. Consequently, it is not yet certain to what extent it can be successfully applied.

The total energy W_t that has been evolved from the beginning of the discharge up to time t is defined by the equation

$$W_t = \int_o^t i\,E\,dt$$

Substituting Eq. [8]

$$W_t = \int_o^t\left[E_s i - K\left(\frac{Q}{Q - it}\right)i^2 - Ni^2 + Ai\exp(-BQ^{-1}it)\right]dt \quad [22]$$

$$W_t = [E_s it + KQi\ln(Q - it) - Ni^2t - AQ/B\exp(-BQ^{-1}it)]_o^t \quad [23]$$

$$W_t = E_s it - KQi\ln(1 - it/Q)^{-1} - Ni^2t + AQ/B(1 - \exp(-BQ^{-1}it)) \quad [24]$$

The constants from an equation describing the discharge of a Ni-Cd cell at 27°C were substituted in Eq. [24] and the total energy evolved at time t was found to be

$$W_t = 1.25\,it - 0.0238\,i\ln(1 - 1.05\,it)^{-1} - 0.006\,i^2t + 0.0248\,[1 - \exp(-3.83\,it)] \quad [25]$$

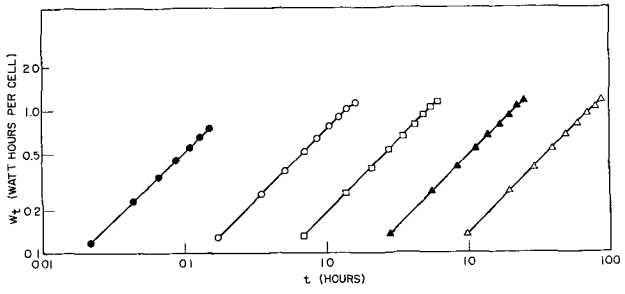

Fig. 8. Comparison of the energy evolved during the discharge of a Ni-Cd cell with the calculated results for various current densities. Sealed nickel cadmium cell, NiOOH-Cd-KOH, 27°C. Calculated points, amp/cell: •, 4.5; ○, 0.56; □, 0.14; ▲, 0.035; △, 0.010.

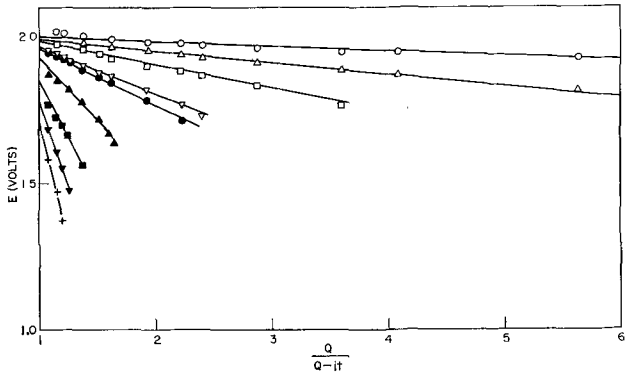

Fig. 9. Discharge curves showing the potential as a function of $Q/Q\text{-}it$ for various current densities. Lead acid cell, PbO_2-Pb-H_2SO_4. Current density, amp/cell: ○, 0.8; △, 2; □, 4; ▽, 8; •, 10; ▲, 20; ■, 40; ▼, 60; +, 80.

In Fig. 8, W_t in watt hours per cell for a Ni-Cd battery has been plotted as a function of t in hours for various values of the cell current in amperes. The solid lines are obtained from calculations based on numerical integration of the actual discharge data. The points are calculated from Eq. [24]. The agreement between the calculated and the measured results in such cases depends entirely upon how well Eq. [9] can be fitted to the original discharge data.

Once the discharge is past the initial potential drop, the exponential term becomes negligible and Eq. [9] can be written as

$$E = E_s - Ni - \left(\frac{Q}{Q - it}\right)Ki \qquad [26]$$

which shows the potential E to be a linear function of $Q/(Q - it)$ with slope $-Ki$ for any given current density, i. Actual discharge potentials were taken from the lead acid battery discharge data in Fig. 4d and plotted in Fig. 9 against $Q/(Q - it)$ for each of nine current densities. Straight lines gave good fits to these plotted points. The average value of the K's, determined from the slopes of each of these nine lines was 0.0195 as compared to the calculated value of 0.0189 given in Table II.

In Fig. 9 the values of E for $Q/(Q - it)$ equals one can be seen from Eq. [26] to be

$$E = E_s - (N + K)i \qquad [27]$$

which shows E here to be a linear function of i with slope, $-(N + K)$, and intercept, E_s. Values of E for $Q/(Q - it)$ equals one were taken from Fig. 9 and plotted in Fig. 10 to give a straight line. The numerical values of E_s and N determined from this straight line were 1.998 and −0.0155 as compared to the calculated values of 2.003 and −0.0150 given in Table II. The values of E_s, K, and N determined by the two methods are virtually identical and show that the graphical

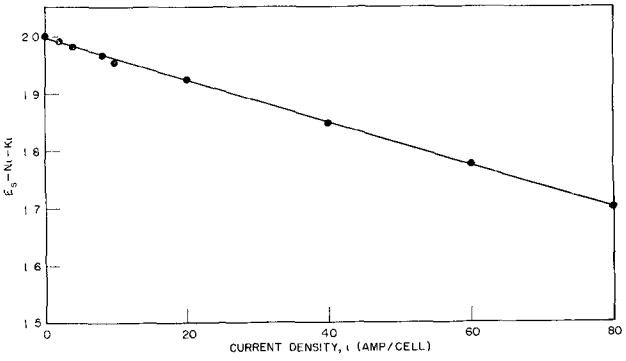

Fig. 10. E_s-Ni-Ki plotted as a function of current density

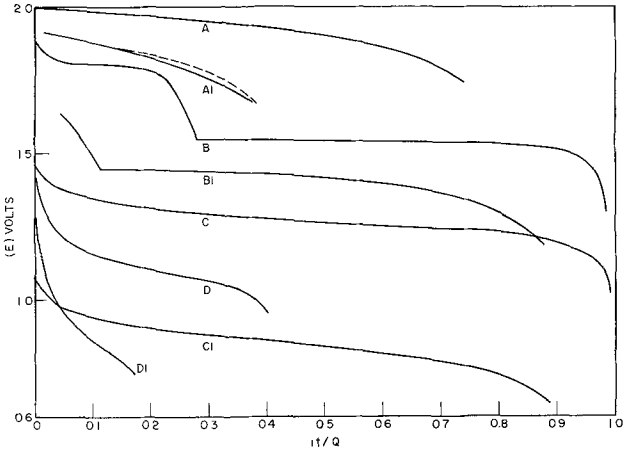

Fig. 11. Discharge curves showing the cell potential during discharge as a function of the fraction of active material used up at any given time.

	Rate Q/i
A, Lead acid	11 hr 14.6 hr
A1, Lead acid	1 hr 2.8 hr
B, Silver zinc	11 hr 11.2 hr
B1, Silver zinc	1 hr 1.14 hr
C, Edison	11 hr 11.3 hr
C1, Edison	1 hr 1.12 hr
D, Dry cell	11 hr 25.6 hr
D1, Dry cell	1 hr 6.4 hr

method of Fig. 9 and 10 can be used in fitting Eq. [9] to discharge data whenever the value of Q is known. If the basic assumption holds true, then Q can be calculated from the amount of active material on the controlling electrode and the graphical method is applicable. In the more empirical applications, such as the lead acid battery just shown, the calculated value of Q will be somewhat less than the value determined from the amount of active material and the graphical method would not be accurate. Almost all of the available discharge data gave no information on the amount of active materials and consequently the feasibility of using this graphical method for fitting Eq. [9] to discharge data has not yet been determined.

Presentation of Discharge Data

A study of Eq. [9] suggests the possibility of plotting battery discharge data against dimensionless quantities in a manner that would make possible more direct comparisons between various types of cells. In Fig. 11 the potential during discharge is plotted as a function of it/Q where it/Q is the fraction of active material used up at time, t. Discharge data are shown here at the 1-hr and the 11-hr rate for four common types of cells. The value of it/Q at the end of the discharge is the efficiency of utilization of the active material. In each case, the discharge was assumed

to be ended when E equalled $E_s - Ki - Ni - 0.25$v. Thus in Fig. 1, curve i_a, the end voltage would be 0.25v below the voltage at point a. A drop of more than 0.25v would have precluded the use of much of the available data. In Fig. 4 the discharge curves are shown as dotted lines wherever they extended past this assumed end point.

Here in Fig. 11 is a method of comparing at equal discharge times such factors as efficiencies, potentials, variations of potentials with time, potential drops due to internal resistance, etc., for various types of constructions of cells. The two curves at A1 represent two different sizes and constructions of lead acid cells. Although the difference in discharge characteristics is small between these two cells, it could, in many cases, be quite large and could be readily demonstrated on a chart of this type. Other things being equal, the cell size is not important here, since each cell is being discharged at a particular value of Q/i that is held constant with change in cell size, which is equivalent to saying n times the current would be drawn from a cell n times as large. The values of Q/i given in Fig. 11 represent the time each cell would have taken to discharge 100% of the active material on the controlling electrode at the particular current density, i. The discharge characteristics of the four cells in Fig. 11 could have been compared by plotting E *vs.* it/Q at a constant value of Q/i such as 10 hr, thus giving a slightly different graph. A number of other variations can be made of this chart. The vertical axis could be the ratio of the discharge potential to the theoretical potential. In this case the area under the curve would be the theoretical watt hour efficiency. If the vertical axis were the ratio of the discharge potential to the average charge voltage, E_c, the area under the curve would be the watt hour efficiency defined by the ratio of the output in watt hours to the input in watt hours. The equation for this latter curve can be obtained by dividing E_c into Eq. [9] to give

$$\left(\frac{E}{E_c}\right) = \left(\frac{E_s}{E_c}\right) - \left(\frac{K}{E_c} i\right)\left[\frac{1}{1 - (it/Q)}\right] - \left(\frac{N}{E_c} i\right) + \left(\frac{A}{E_c}\right)[\exp(-BQ^{-1})(it)] \quad [28]$$

where each quantity in brackets or parentheses is dimensionless. In Fig. 11 the values of it/Q were taken from Table II and are empirical to a certain extent. If Q had been calculated from the actual amounts of active material on the controlling electrode, its value would have been slightly larger and the discharge curves in Fig. 11 would be changed slightly. Values of (it) per unit weight of active material or per unit cell weight, or watt hour efficiencies could have been used in place of it/Q for the abscissa in Fig. 11. The important thing in each of these cases is that the use of some form of dimensionless quantity, or factor closely related thereto, as either or both of the coordinates enables a quantitative, visual study and comparison to be made of the characteristics of certain types of equivalent discharges, either for different types of cell systems, or different constructions of the same cell system, or both. As shown in Eq. [28], the equation for each of these cases can be obtained easily from Eq. [9].

Manuscript received Feb. 4, 1965. This paper was presented at the Boston Meeting, Sept. 16-20, 1962.

Any discussion of this paper will appear in a Discussion Section to be published in the June 1966 JOURNAL.

REFERENCES

1. C. F. Anderson, *This Journal*, **99**, 244C (1952).
2. C. P. Wales, NRL Rpt 5167, 11 Aug. 1958.
3. E. A. Hoxie, *Trans.*, AIEE, Part II Applications and Industry, **73**, 17 (1954).
4. G. B. Ellis, H. Mandel, and D. Linden, *This Journal*, **99**, 250C (1952).
5. W. J. Schlotter, *ibid.*, **99**, 205C (1952).

GLOSSARY

A	Numerical value of Δe at $(it) = 0$ (v)
α	Transfer coefficient (dimensionless)
B	Constant parameter (dimensionless)
C	Constant parameter (volt cm^2 amp^{-1} sec^{-1})
E	Cell potential during discharge (v)
E_a	Anode potential during discharge (v)
E_c	Cathode potential during discharge (v)
E_s	A constant potential parameter (v)
ΔE	Initial potential drop (v)
η	Steady-state activation overpotential (v)
F	Faraday (coulombs equiv.$^{-1}$)
i	Apparent current density (amp cm^{-2})
i_{am}	Active material current density (amp cm^{-2})
i_o	Apparent exchange current density (amp cm^{-2})
K	Coefficient of polarization (ohm cm^2)
K_a	Coefficient of polarization for anode (ohm cm^2)
K_c	Coefficient of polarization for cathode (ohm cm^2)
N	Internal resistance of cell (ohm cm^2)
Q	Amount of active material on controlling electrode as coulombs (coulombs cm^{-2})
Q_a	Amount of active material on anode as coulombs (coulombs cm^{-2})
Q_c	Amount of active material on cathode as (coulombs cm^{-2})
R	Gas constant (amp volt sec deg^{-1} mole^{-1})
T	Temperature (deg)
t	Time (min or hr)
W_t	Energy evolved during cell discharge (amp volt sec cm^{-2})
Z	Number of electrons transferred in rate determining step (dimensionless)